27th ABCM International Congress of Mechanical Engineering
December 04-08, 2023, Florianópolis-SC, Brazil

COB-2023-1433
ROBUST UAV FORMATION CONTROL

Thamiris Costa
Federal University of Santa Catarina, Automation and Systems Department, Florianópolis, Santa Catarina, Brazil
thamiriscosta@gmail.com

Ebrahim El'Youssef
Federal University of Santa Catarina, Automation and Control Engineering and Computation Department, Blumenau, Santa Catarina, Brazil
ebrahim.el.youssef@ufsc.br

Edson De Pieri
Federal University of Santa Catarina, Automation and Systems Department, Florianópolis, Santa Catarina, Brazil
edson.pieri@ufsc.br

Abstract. *The formation control problem consists of formulating a control law capable of maintaining the UAVs at a safe distance from each other, controlling the UAVs in their desired positions during the entire task execution time, and ensuring that the UAVs will not collide with each other. Thus, proposing a solution for the formation control problem involves different technological challenges, implying an active research topic. Then, the work aims to develop a robust formation control based on the robust control H_∞ methodology for a multi-UAV system composed by UAVs with tilt rotors. The approaches used to develop the control system are the leader-follower and consensus. The control law is obtained considering the methodology of the robust control H_∞. The stability analysis uses the Lyapunov theory through linear matrix inequalities (LMIs). The results were analyzed through numerical simulations considering a multi-UAV composed of two virtual leaders and six followers. In the results, it is possible to verify that the formation could keep the desired shape during the task execution time. Then, the control system proposed could lead to the work objective achievement.*

Keywords: *UAVs, Formation control, Robust controller.*

1. INTRODUCTION

Unmanned aerial vehicles (UAVs) have been attracting the attention of researchers because of the many advantages they offer in various domains. These aerial robots enable access to locations otherwise unreachable to humans, whether because of security concerns or inaccessibility. While UAV systems already possess inherent advantages, leveraging multiple UAVs collaboratively in the same task brings further benefits, including enhanced fault tolerance, flexibility, and time efficiency.

The study of multi-UAV systems is a prominent research topic that has received extensive attention. These systems are inherently complex and encompass various technological challenges. Developing multi-UAV systems involves addressing decision-making, path planning, control, and communication subsystems. This work specifically focuses on the control aspect. Controlling multi-UAV systems entails managing formation control, which pertains to effectively shaping the UAVs to track desired positions or trajectories.

Various approaches have been employed to address the formation control problem, including virtual-structure (Liu *et al.*, 2019, 2020), leader-follower (Dong *et al.*, 2016; He *et al.*, 2018; Ai and Yu, 2019; Dong *et al.*, 2018; Yan and Ma, 2020; Kartal *et al.*, 2020; Wang *et al.*, 2021), behavior-based (Oh *et al.*, 2017), and consensus methods (He *et al.*, 2018; Liu *et al.*, 2019; Wang *et al.*, 2021).

The virtual-structure approach utilizes a guiding virtual structure to ensure all agents meet formation constraints. Similarly, the leader-follower approach designates a leader to fulfill this role. While both methods require complete information about the virtual structure or leader, respectively, they offer good control capabilities and are widely utilized. However, they need more inflexibility, posing challenges for formation members to navigate around obstacles.

In contrast, the behavior-based strategy establishes desired behaviors for formation agents, including collision avoidance, formation reconfiguration, formation maintenance, and trajectory tracking (Oh *et al.*, 2015; Yang and Hu, 2020). This approach adapts well to environmental changes due to its behavioral foundation. Additionally, the computational complexity remains the same with the addition of more robots since agents do not require global interaction. However, stability analysis becomes complex as this control strategy relies on something other than the system's kinematics or dynamics (Ahn, 2020).

Another widely employed approach is the consensus algorithm, which coordinates the states of individual agents to reach a consensus on a variable of interest. Position and velocity coordination are used to achieve consensus and maintain the desired structure (Yang and Hu, 2020; Wu *et al.*, 2021).

Besides achieving and maintaining the desired formation, the robustness of a control system is crucial because of the presence of unmodeled dynamics and unstructured perturbations commonly encountered in real-world environments. Therefore, it is desirable to formulate control laws that provide robustness guarantees. The utilization of robust control methodologies in formulating control laws holds significant promise.

This research aims to address the formation control problem for UAVs with tilt rotors, which are presented in the previous works (Vendrichoski *et al.*, 2019; Costa *et al.*, 2019, 2021). To accomplish this, we propose a robust formation control strategy for a multi-UAV system, incorporating both the leader-follower and consensus approaches. Combining these methodologies can enhance the system's response, leading to improved convergence. The control law is obtained using the robust control methodology known as H_∞ to ensure the stability of the system even in the presence of unmodeled dynamics. For the result analysis, we consider two virtual leaders, each governing a group comprising three agents.

To the best of our knowledge, developing a robust formation control framework integrating leader-follower, consensus, and H_∞ robust control methodologies for a group of UAVs with tilt rotors has yet to be explored. Thus, the main contribution of this study lies in the development of a robust formation control scheme that integrates both leader-follower and consensus methodologies while employing the H_∞ approach to derive the control law for a multi-UAV system with tilt rotors.

The rest of this paper is organized as follows. In Section 2, we present preliminary concepts. We present the formation control design in Section 3. We present the numerical simulation results in Section 4. In Section 5, we present the work conclusion and future works.

2. PRELIMINAIRES

This section provides an introduction to the foundational concepts necessary for developing the formation control system. First, we present the graph theory, which plays an important role in modeling the communication flow within the system. Subsequently, we present the system model, outlining its key components and dynamics. Finally, we proceed with the formulation of the formation control problem.

Throughout this study, a specific notation is adopted for clarity and consistency. Lowercase letters denote constants, lowercase bold letters signify vectors, and uppercase letters denote matrices.

2.1 Graph theory

A graph representing a multi-agent system composed of N agents is described by the triple $G = (\mathcal{V}, \mathcal{E}, \mathcal{W})$, where $\mathcal{V} = \{\mathfrak{v}_1, \mathfrak{v}_2, \ldots, \mathfrak{v}_N\}$ is the vertices set, $\mathcal{E} \subseteq \{e_{ij} = (\mathfrak{v}_i, \mathfrak{v}_j) : \mathfrak{v}_i, \mathfrak{v}_j \in \mathcal{V}; i \neq j\}$ is the edges set, and $\mathcal{W} = \begin{bmatrix} w_{ij} \end{bmatrix} \in \mathbb{R}^{N \times N}$ is the weighted adjacency matrix, with $w_{ii} = 0$, $w_{ij} > 0$, if $(i, j) \in \mathcal{E}$ and $w_{ij} = 0$, otherwise. The graph is called an undirected graph if $w_{ij} = w_{ji}$, and it is called a directed graph if $w_{ij} > 0$, and $w_{ji} = 0$. Also, two vertices or nodes are called neighbors if there is an edge connecting both, i.e., $\mathfrak{v}_i \in \mathcal{V}$ and $\mathfrak{v}_j \in \mathcal{V}$ are neighbors if $e_{ij} \neq 0$.

The information exchange among the agents is described by the graph representation, where each vertices represents each agent and the existence of communication among two agents by an edge. The Laplacian matrix $\mathcal{L} \in \mathbb{R}^{N \times N}$ is given by $l_{ii} = \sum_{j=1, j\neq i}^{N} w_{ij}$, and $l_{ij} = -w_{ij}$, for $i \neq j, \forall i, j \in \{1, 2, \ldots, N\}$ (Ahn, 2020).

A graph G is assumed to be connected if a path connects any node to another within the graph. A root is defined as a node without a parent, i.e., a node that does not receive any information from another node. A tree is characterized as a directed graph possessing a root, with the remaining nodes having only one parent each. A spanning tree of a graph G is a tree that includes all nodes present in G. Concerning multi-agent systems, consensus is achieved when the graph representing the information flow between the agents possesses a spanning tree (Ahn, 2020).

2.2 Model

The UAV considered in this work is based on the quadrotor with tilt rotors discussed in the previous work (Vendrichoski *et al.*, 2019). Fig. 1 depicts the UAV's configuration.

The mathematical representation of a UAV's dynamics is a complex nonlinear model, as it is described in (Vendrichoski *et al.*, 2019). To simplify the development of the control system, we separate the translation and rotation dynamics. This separation is because of the significant difference in time constants between the two dynamics, i.e. the time constant of the rotation dynamics is much smaller than translation (Mo and Farid, 2019). The resulting cascade control system comprises an outer loop for the translation dynamics and an inner loop for the rotation.

In multi-UAV systems, the formation control is implemented in the outer loop, while the inner loop focuses on the rotational dynamics, as it is presented in Fig. 2.

The UAVs dynamics models and the altitude and attitude controllers used in this work are based on the ones presented

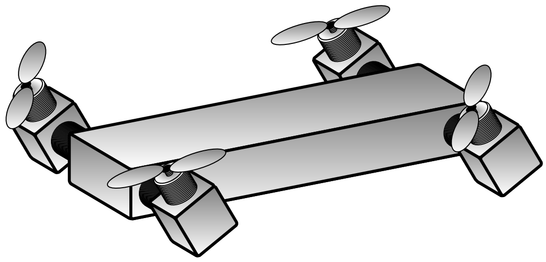

Figure 1. Quadrotor with tilt rotors.

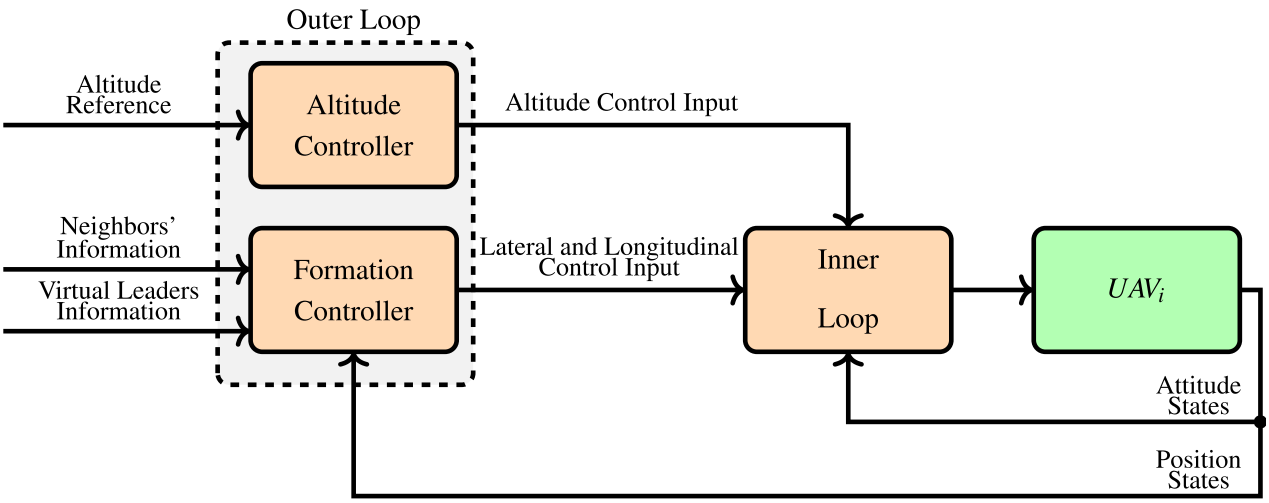

Figure 2. UAVs' block diagram.

in the previous works Vendrichoski *et al.* (2019); Costa *et al.* (2021). The altitude controller was developed using the PID methodology, while the attitude controller was formulated by using the Generalized Super-Twisting Sliding Mode Control approach (GSTSMC).

To formulate the formation control, we consider the position dynamics as a double-integrator model given by

$$\begin{cases} \dot{\boldsymbol{p}}_{\boldsymbol{i}}(t) &= \boldsymbol{v}_{\boldsymbol{i}}(t), \\ \dot{\boldsymbol{v}}_{\boldsymbol{i}}(t) &= \boldsymbol{u}_{\boldsymbol{i}}(t), \end{cases} \tag{1}$$

where $\boldsymbol{p}_{\boldsymbol{i}}(t) \in \mathbb{R}^{n\times 1}$ is the position vector, $\boldsymbol{v}_{\boldsymbol{i}} \in \mathbb{R}^{n\times 1}$ is the velocity error, and $\boldsymbol{u}_{\boldsymbol{i}} \in \mathbb{R}^{n\times 1}$ is the control input, for $i = 1, \ldots, N$.

2.3 Problem formulation

The objective is to maneuver a multi-UAV system in three-dimensional space, with each UAV tracking the position of a virtual leader. The UAVs maintain a specific relative lateral and longitudinal distance to the leader while staying at the same altitude, thus maintaining the desired formation.

The virtual leaders positions and velocities are given by $\boldsymbol{p}_{\boldsymbol{vl_1}}(t) \in \mathbb{R}^{n\times 1}$, $\boldsymbol{p}_{\boldsymbol{vl_2}}(t) \in \mathbb{R}^{n\times 1}$, $\boldsymbol{v}_{\boldsymbol{vl_1}} \in \mathbb{R}^{n\times 1}$, and $\boldsymbol{v}_{\boldsymbol{vl_2}} \in \mathbb{R}^{n\times 1}$, respectively, with $\dot{\boldsymbol{p}}_{\boldsymbol{vl_1}} = \boldsymbol{v}_{\boldsymbol{vl_1}}$, $\dot{\boldsymbol{p}}_{\boldsymbol{vl_2}} = \boldsymbol{v}_{\boldsymbol{vl_2}}$, $\dot{\boldsymbol{v}}_{\boldsymbol{vl_1}} = \dot{\boldsymbol{v}}_{\boldsymbol{vl_2}} = \mathbb{O}_{n\times 1}$. The vector gives the relative position between the virtual leaders and the followers $\boldsymbol{h}_{\boldsymbol{p_i}} \in \mathbb{R}^{n\times 1}$, for $i = 1, \ldots, N$.

3. FORMATION CONTROL DESIGN

Consider as states vector of the UAV i is defined as $\boldsymbol{\xi}_{\boldsymbol{i}}(t) = \begin{bmatrix} \boldsymbol{p}_{\boldsymbol{i}}^T & \boldsymbol{v}_{\boldsymbol{i}}^T \end{bmatrix}^T \in \mathbb{R}^{2n\times 1}$, $\boldsymbol{\xi}_{\boldsymbol{vl_1}}(t) = \begin{bmatrix} \boldsymbol{p}_{\boldsymbol{vl_1}}^T & \boldsymbol{v}_{\boldsymbol{vl_1}}^T \end{bmatrix}^T \in \mathbb{R}^{2n\times 1}$, $\boldsymbol{\xi}_{\boldsymbol{vl_2}}(t) = \begin{bmatrix} \boldsymbol{p}_{\boldsymbol{vl_2}}^T & \boldsymbol{v}_{\boldsymbol{vl_2}}^T \end{bmatrix}^T \in \mathbb{R}^{2n\times 1}$, $\boldsymbol{h}_{\boldsymbol{i}} = \begin{bmatrix} \boldsymbol{h}_{\boldsymbol{p_i}}^T & \mathbb{O}_{1\times n} \end{bmatrix}^T \in \mathbb{R}^{2n\times 1}$. Defining the error vector $\tilde{\boldsymbol{\xi}}_{\boldsymbol{i}} = \boldsymbol{\xi}_{\boldsymbol{i}} - \boldsymbol{\xi}_{\boldsymbol{vl_i}} - \boldsymbol{h}_{\boldsymbol{i}} \in \mathbb{R}^{2n\times 1}$, and considering the action of unstructured disturbances, the error model is given by

$$\begin{aligned}\dot{\tilde{\boldsymbol{\xi}}}_{\boldsymbol{i}}(t) &= \boldsymbol{A}\tilde{\boldsymbol{\xi}}_{\boldsymbol{i}}(t)+\boldsymbol{B}\boldsymbol{u}_{\boldsymbol{i}}(t)+\boldsymbol{B}_{\boldsymbol{d}}\boldsymbol{\Omega}_{\boldsymbol{i}}(t)\\ \boldsymbol{z}_{\boldsymbol{i}}(t) &= \boldsymbol{C}\tilde{\boldsymbol{\xi}}_{\boldsymbol{i}}(t)+\boldsymbol{D}\boldsymbol{u}_{\boldsymbol{i}}(t)+\boldsymbol{D}_{\boldsymbol{d}}\boldsymbol{\Omega}_{\boldsymbol{i}}(t),\end{aligned} \tag{2}$$

with

$$\boldsymbol{A}=\begin{bmatrix}\mathbb{O}_{n\times n} & \mathbb{I}_{n\times n}\\ \mathbb{O}_{n\times n} & \mathbb{O}_{n\times n}\end{bmatrix},\quad \boldsymbol{B}=\begin{bmatrix}\mathbb{O}_{n\times n} & \mathbb{I}_{n\times n}\\ \mathbb{O}_{n\times n} & \mathbb{O}_{n\times n}\end{bmatrix},\quad \boldsymbol{B_d}=\begin{bmatrix}\mathbb{O}_{n\times n} & \mathbb{I}_{n\times n}\\ \mathbb{O}_{n\times n} & \mathbb{O}_{n\times n}\end{bmatrix},$$

and where(t) $\boldsymbol{z_i} \in \mathbb{R}^{n\times 1}$ is the system output for disturbance input, which is represented by $\boldsymbol{\Omega_i}(t) \in \mathbb{R}^{n\times 1}$. $\boldsymbol{C} \in \mathbb{R}^{2n\times 2n}$, $\boldsymbol{D} \in \mathbb{R}^{2n\times n}$, and $\boldsymbol{D_d} \in \mathbb{R}^{2n\times n}$ are matrices defined by the designer during the robust control H_∞ development. To obtain the model of the whole multi-agent system, we define the vector $\tilde{\boldsymbol{\xi}} = \begin{bmatrix}\tilde{\boldsymbol{\xi}}_{\boldsymbol{1}}^T & \dots & \tilde{\boldsymbol{\xi}}_{\boldsymbol{N}}^T\end{bmatrix}^T$ and we obtain

$$\begin{aligned}\dot{\tilde{\boldsymbol{\xi}}}(t) &= (\mathbb{I}_N\otimes\boldsymbol{A})\,\tilde{\boldsymbol{\xi}}(t)+(\mathbb{I}_N\otimes\boldsymbol{B})\,\boldsymbol{u}(t)+(\mathbb{I}_N\otimes\boldsymbol{B_d})\,\boldsymbol{\Omega}(t)\\ \boldsymbol{z}(t) &= (\mathbb{I}_N\otimes\boldsymbol{C})\,\tilde{\boldsymbol{\xi}}(t)+(\mathbb{I}_N\otimes\boldsymbol{D})\,\boldsymbol{u}(t)+(\mathbb{I}_N\otimes\boldsymbol{D_d})\,\boldsymbol{\Omega}(t),\end{aligned} \tag{3}$$

where $\otimes$ indicates the Kronecker product. In the following, we omit the term (t) to simplify the notation.

The formation control law proposed in this work combines leader-follower and consensus methodologies. Then, we formulate

$$\boldsymbol{u_i}=\theta_i\boldsymbol{K_r}\tilde{\boldsymbol{\xi}}_{\boldsymbol{i}}+\sum_{j=1}^{N}w_{ij}\boldsymbol{K_c}\left(\tilde{\boldsymbol{\xi}}_{\boldsymbol{i}}-\tilde{\boldsymbol{\xi}}_{\boldsymbol{j}}\right), \tag{4}$$

for $i = 1,\dots,N$, where the first term in the right-hand side is responsible for the virtual leader trajectory tracking, while the second term corresponds to the consensus control. Also, $\boldsymbol{K_r}, \boldsymbol{K_c} \in \mathbb{R}^{n\times 2n}$ are the trajectory tracking and the consensus gains, respectively. The parameter θ_i indicates if the UAV i has the information about the leader, then $\theta_i = 1$ if it receives the information and $\theta_i = 0$, otherwise. The control law of the multi-UAV system is equal to

$$\boldsymbol{u}=(\boldsymbol{\Theta_N}\otimes\boldsymbol{K_r}+\boldsymbol{L}\otimes\boldsymbol{K_c})\,\tilde{\boldsymbol{\xi}}, \tag{5}$$

where $\boldsymbol{\Theta_N} = diag\,(\theta_1,\dots,\theta_N) \in \mathbb{R}^{N\times N}$, and $\boldsymbol{L} \in \mathbb{R}^{N\times N}$ is the Laplacian matrix.

Being the control law (5) and the error model (3), the closed-loop system is given by

$$\begin{aligned}\dot{\tilde{\boldsymbol{\xi}}} &= (\mathbb{I}_N\otimes\boldsymbol{A}+\boldsymbol{\Theta_N}\otimes\boldsymbol{BK_r}+\boldsymbol{L}\otimes\boldsymbol{BK_c})\,\tilde{\boldsymbol{\xi}}+(\mathbb{I}_N\otimes\boldsymbol{B_d})\,\boldsymbol{\Omega}\\ \boldsymbol{z} &= (\mathbb{I}_N\otimes\boldsymbol{C}+\boldsymbol{\Theta_N}\otimes\boldsymbol{DK_r}+\boldsymbol{L}\otimes\boldsymbol{DK_c})\,\tilde{\boldsymbol{\xi}}+(\mathbb{I}_N\otimes\boldsymbol{D_d})\,\boldsymbol{\Omega}.\end{aligned} \tag{6}$$

To design the gains $\boldsymbol{K_r}$ and $\boldsymbol{K_c}$ to obtain a closed-loop system stable and robust against unstructured dynamics, such as unmodeled dynamics, we propose the Theorem 1.

Theorem 1. *Being μ the characterization of the $\|H\|_\infty$, and G the graph representing the communication of a multi-UAV system, it achieves the desired formation if the graph G has a spanning tree, and if it exists $\boldsymbol{J} = \boldsymbol{J}^T > 0$, such that the following optimization problem is feasible.*

$$\textit{minimize}\qquad \mu \tag{7}$$

$$\mu,\ \boldsymbol{J},\ \boldsymbol{Y_r},\ \boldsymbol{Y_c} \tag{8}$$

$$\boldsymbol{J}>0 \tag{9}$$

$$\begin{bmatrix}\mathbb{I}_N\otimes\left(\boldsymbol{AJ}+\boldsymbol{JA}^T\right)+\boldsymbol{\Theta}_{\boldsymbol{N}}^T\otimes\boldsymbol{Y}_{\boldsymbol{r}}^T\boldsymbol{B}^T+\boldsymbol{\Theta_N}\otimes\boldsymbol{BY_r}+\boldsymbol{L}^T\otimes\boldsymbol{Y}_{\boldsymbol{c}}^T\boldsymbol{B}^T+\boldsymbol{L}\otimes\boldsymbol{BY_c} & \dots\\ \mathbb{I}_N\otimes\boldsymbol{B}_{\boldsymbol{d}}^T & \dots\\ \mathbb{I}_N\otimes\boldsymbol{CJ}+\boldsymbol{\Theta_N}\otimes\boldsymbol{DY_r}+\boldsymbol{L}\otimes\boldsymbol{DY_c} & \dots\end{bmatrix} \tag{10}$$

$$\begin{matrix}\dots & \mathbb{I}_N\otimes\boldsymbol{B_d} & \mathbb{I}_N\otimes\boldsymbol{JC}^T+\boldsymbol{\Theta_N}\otimes\boldsymbol{Y}_{\boldsymbol{r}}^T\boldsymbol{D}^T+\boldsymbol{L}^T\otimes\boldsymbol{Y}_{\boldsymbol{c}}^T\boldsymbol{D}^T\\ \dots & -\mathbb{I}_N\otimes\mu\mathbb{I}_{n\times n} & \mathbb{I}_N\otimes\boldsymbol{D}_{\boldsymbol{d}}^T\\ \dots & \mathbb{I}_N\otimes\boldsymbol{D_d} & \mathbb{I}_{2n\times 2n}\end{matrix}\Bigg] < 0 \tag{11}$$

Therefore, the gains are obtained by

$$\boldsymbol{K_r} = \boldsymbol{Y_r J}^{-1}, \tag{12}$$
$$\boldsymbol{K_c} = \boldsymbol{Y_c J}^{-1}, \tag{13}$$
$$\tag{14}$$

and the $\|H\|_\infty$ is given by

$$\gamma = \sqrt{\mu}. \tag{15}$$

Proof. To verify the stability of Eq. (6), consider the Lyapunov function

$$V = \tilde{\boldsymbol{\xi}}^T \left(\mathbb{I}_N \otimes \boldsymbol{P}\right) \tilde{\boldsymbol{\xi}}, \tag{16}$$

where $\boldsymbol{P} = \boldsymbol{P}^T > 0 \in \mathbb{R}^{2n\times 2n}$ is the Lyapunov matrix. To verify the stability, the derivative of (16) must be negative defined. Then, deriving with respect to time, we have

$$\dot{V} = \dot{\tilde{\boldsymbol{\xi}}}^T \left(\mathbb{I}_N \otimes \boldsymbol{P}\right) \tilde{\boldsymbol{\xi}} + \tilde{\boldsymbol{\xi}}^T \left(\mathbb{I}_N \otimes \boldsymbol{P}\right) \dot{\tilde{\boldsymbol{\xi}}} < 0. \tag{17}$$

To be robust to unstructured disturbances, like unmodeled dynamics, we consider the norm H_∞ in the stability analysis. Being $H(s)$, the transfer function relating the input $\boldsymbol{\Omega}$ with the output $\boldsymbol{z}$, the norm H_∞ is characterized as

$$\|H\|_\infty = sup \frac{\|\boldsymbol{z}\|_2}{\|\boldsymbol{\Omega}\|_2} \leq \gamma^2. \tag{18}$$

Considering (17) and (18), we have the following condition

$$\dot{\tilde{\boldsymbol{\xi}}}^T \left(\mathbb{I}_N \otimes \boldsymbol{P}\right) \tilde{\boldsymbol{\xi}} + \tilde{\boldsymbol{\xi}}^T \left(\mathbb{I}_N \otimes \boldsymbol{P}\right) \dot{\tilde{\boldsymbol{\xi}}} + \boldsymbol{z}^T\boldsymbol{z} - \gamma^2 \boldsymbol{\Omega}^T\boldsymbol{\Omega} < 0. \tag{19}$$

Replacing the closed-loop system (6) in (19), it is obtained

$$\begin{bmatrix} \tilde{\boldsymbol{\xi}}^T & \boldsymbol{\Omega}^T \end{bmatrix} \boldsymbol{M} \begin{bmatrix} \tilde{\boldsymbol{\xi}} \\ \boldsymbol{\Omega} \end{bmatrix} < 0, \tag{20}$$

with

$$\boldsymbol{M} = \begin{bmatrix} M_{11} & M_{12} \\ * & M_{22} \end{bmatrix},$$

where $*$ represents symmetric elements, and

$$\begin{aligned}
M_{11} = {} & \mathbb{I}_N \otimes \boldsymbol{A}^T\boldsymbol{P} + \beta_N^T \otimes \boldsymbol{K_r}^T\boldsymbol{B}^T\boldsymbol{P} + \boldsymbol{L}^T \otimes \boldsymbol{K_c}^T\boldsymbol{B}^T\boldsymbol{P} + \mathbb{I}_N \otimes \boldsymbol{PA} + \boldsymbol{\beta}_N \otimes \boldsymbol{PBK_r} + \boldsymbol{L} \otimes \boldsymbol{PBK_c} + \\
& + \mathbb{I}_N \otimes \boldsymbol{C}^T\boldsymbol{C} + \boldsymbol{\beta} \otimes \boldsymbol{C}^T\boldsymbol{DK_r} + \boldsymbol{L} \otimes \boldsymbol{C}^T\boldsymbol{DK_c} + \boldsymbol{\beta}^T \otimes \boldsymbol{K_r}^T\boldsymbol{D}^T\boldsymbol{C} + \boldsymbol{\beta}^T\boldsymbol{\beta} \otimes \boldsymbol{K_r}\boldsymbol{D}^T\boldsymbol{DK_r} + \\
& + \boldsymbol{\beta}^T\boldsymbol{L} \otimes \boldsymbol{K_r}\boldsymbol{D}^T\boldsymbol{DK_c} + \boldsymbol{L}^T \otimes \boldsymbol{K_c}^T\boldsymbol{D}^T\boldsymbol{C} + \boldsymbol{L}^T\boldsymbol{\beta} \otimes \boldsymbol{K_c}^T\boldsymbol{D}^T\boldsymbol{DK_r} + \boldsymbol{L}^T\boldsymbol{\beta} \otimes \boldsymbol{K_c}^T\boldsymbol{D}^T\boldsymbol{DK_c}, \\
M_{12} = {} & \mathbb{I}_N \otimes \boldsymbol{C}^T\boldsymbol{D_d} + \boldsymbol{\beta}^T \otimes \boldsymbol{K_r}^T\boldsymbol{D}^T\boldsymbol{D_d} + \boldsymbol{L}^T \otimes \boldsymbol{K_c}^T\boldsymbol{D}^T\boldsymbol{D_d}, \\
M_{22} = {} & \mathbb{I}_N \otimes \boldsymbol{D_d}^T\boldsymbol{D_d} - \mathbb{I}_N \otimes \gamma^2.
\end{aligned}$$

The condition in Eq. (20) is definite negative if the matrix $\boldsymbol{M}$ is definite negative. Also, the matrix $\boldsymbol{M}$ is nonlinear due to the multiplication of the unknown variables $\boldsymbol{P}$, $\boldsymbol{K_r}$, and $\boldsymbol{K_c}$, motivating the mathematical manipulations performed to obtain a linear matrix inequality.

First, we pre and post-multiply the matrix M by

$$\begin{bmatrix} \mathbb{I} \otimes \boldsymbol{P}^{-1} & \mathbb{I} \otimes \mathbb{O}_{2n\times 2n} \\ \mathbb{I} \otimes \mathbb{O}_{2n\times 2n} & \mathbb{I} \otimes \mathbb{I}_{2n\times 2n} \end{bmatrix},$$

to group the unknown variables. In the following, we apply the Schur Complement and make the variables change

$$\mu = \gamma^2, \tag{21}$$
$$\boldsymbol{J} = \boldsymbol{P}^{-1}, \tag{22}$$
$$\boldsymbol{Y_r} = \boldsymbol{K_r}\boldsymbol{P}^{-1}, \tag{23}$$
$$\boldsymbol{Y_c} = \boldsymbol{K_c}\boldsymbol{P}^{-1}, \tag{24}$$

obtaining the following LMI

$$\begin{bmatrix} \mathbb{I}_N \otimes \left(\boldsymbol{AJ} + \boldsymbol{JA}^T\right) + \boldsymbol{\Theta_N}^T \otimes \boldsymbol{Y_r}^T\boldsymbol{B}^T + \boldsymbol{\Theta_N} \otimes \boldsymbol{BY_r} + \boldsymbol{L}^T \otimes \boldsymbol{Y_c}^T\boldsymbol{B}^T + \boldsymbol{L} \otimes \boldsymbol{BY_c} & \dots \\ \mathbb{I}_N \otimes \boldsymbol{B_d}^T & \dots \\ \mathbb{I}_N \otimes \boldsymbol{CJ} + \boldsymbol{\Theta_N} \otimes \boldsymbol{DY_r} + \boldsymbol{L} \otimes \boldsymbol{DY_c} & \dots \end{bmatrix}$$

$$\begin{bmatrix} \dots & \mathbb{I}_N \otimes \boldsymbol{B_d} & \mathbb{I}_N \otimes \boldsymbol{JC}^T + \boldsymbol{\Theta_N} \otimes \boldsymbol{Y_r}^T\boldsymbol{D}^T + \boldsymbol{L}^T \otimes \boldsymbol{Y_c}^T\boldsymbol{D}^T \\ \dots & -\mathbb{I}_N \otimes \mu\mathbb{I}_{n\times n} & \mathbb{I}_N \otimes \boldsymbol{D_d}^T \\ \dots & \mathbb{I}_N \otimes \boldsymbol{D_d} & \mathbb{I}_{2n\times 2n} \end{bmatrix} < 0.$$

□

4. RESULTS

A simulation was conducted using a complete dynamic model of six UAVs with tilt rotors developed in the previous work (Vendrichoski *et al.*, 2019). Each UAV's control system comprises an outer loop for the formation control developed in this work, a PID controller for altitude control, and an inner loop for the attitude controller and rotors' inclination controller designed using the GSTSMC. The PID and the GSTSMC controllers were developed in (Costa *et al.*, 2021). The propellers' force is subject to saturation, limited to the range of $(0,\ 20)\ N$, and the rotors' inclination is limited to the range $(-5,\ 5)\ N.m$.

The multi-UAV system is divided into two groups, each governed by a virtual leader, as presented in Fig. 3. The groups can communicate to ensure consensus while executing a task.

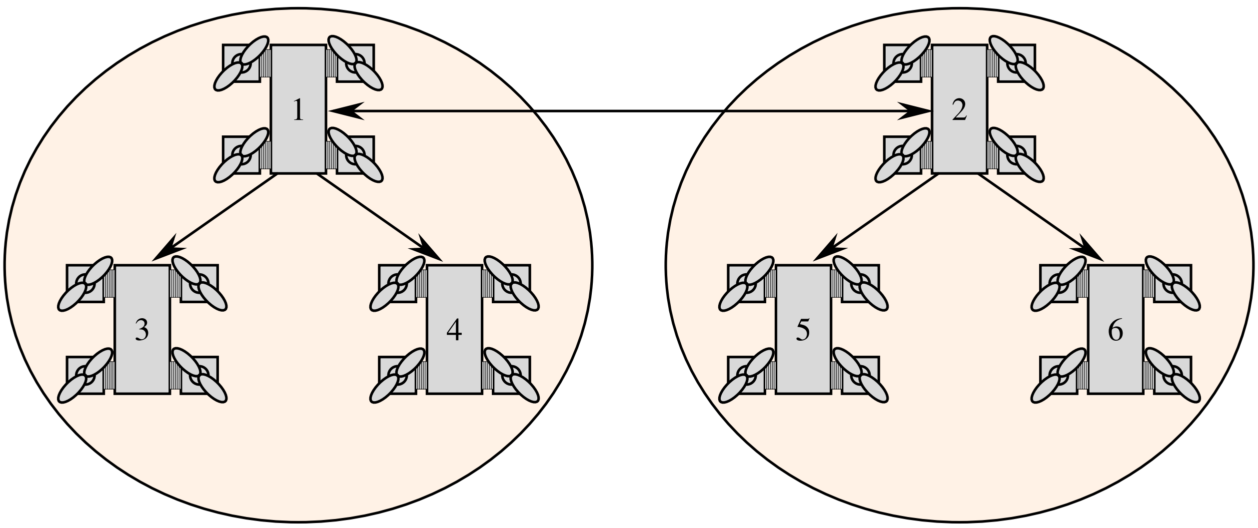

Figure 3. UAVs' formation shape.

The UAVs 1 and 2 have access to the information of the virtual leaders 1 and 2, respectively. The UAVs 3 and 4 receive the information of the UAV 1, and the UAVs 5 and 6 receive the information of the UAV 2. Also, the UAVs 1, and 2 can communicate. The edges set of the graph G is given vy $\mathcal{E} = \{(\mathfrak{v}_1, \mathfrak{v}_2), (\mathfrak{v}_2, \mathfrak{v}_1), (\mathfrak{v}_3, \mathfrak{v}_1), (\mathfrak{v}_4, \mathfrak{v}_1), \{(\mathfrak{v}_5, \mathfrak{v}_2), (\mathfrak{v}_6, \mathfrak{v}_2)\}$. The trajectories of the virtual leaders are equal to $\boldsymbol{p_{vl_1}} = \begin{bmatrix} t & 0.2t \end{bmatrix}^T$, and $\boldsymbol{p_{vl_2}} = \begin{bmatrix} t+7 & 0.2t-1 \end{bmatrix}^T$, and the desired relative distance of the virtual leader is given by $\boldsymbol{h_1} = \begin{bmatrix} 0 & 0 \end{bmatrix}^T$, $\boldsymbol{h_2} = \begin{bmatrix} 0 & 0 \end{bmatrix}^T$, $\boldsymbol{h_3} = \begin{bmatrix} -1 & -1 \end{bmatrix}^T$, $\boldsymbol{h_4} = \begin{bmatrix} 1 & -1 \end{bmatrix}^T$, $\boldsymbol{h_5} = \begin{bmatrix} -1 & -1 \end{bmatrix}^T$, and $\boldsymbol{h_6} = \begin{bmatrix} 1 & -1 \end{bmatrix}^T$.

The gains of the formation control law in Eq. (5) were obtained by finding a solution for the optimization problem presented in Theorem 1. The problem was solved in the MATLAB software using the toolbox YALMIP and Sedumi. The gains obtained are equal to

$$\boldsymbol{K_r} = \begin{bmatrix} -1.4428 & 0 & -13.0127 & 0 \\ 0 & -1.4428 & 0 & -13.0127 \end{bmatrix}, \tag{25}$$

$$\boldsymbol{K_c} = \begin{bmatrix} -0.5660 & 0 & -5.1050 & 0 \\ 0 & -0.5660 & 0 & -5.1050 \end{bmatrix}. \tag{26}$$

The trajectory of the agents is illustrated in Fig. 4. It can be observed that the UAVs tracked the virtual leaders' trajectories while maintaining the specified offsets.

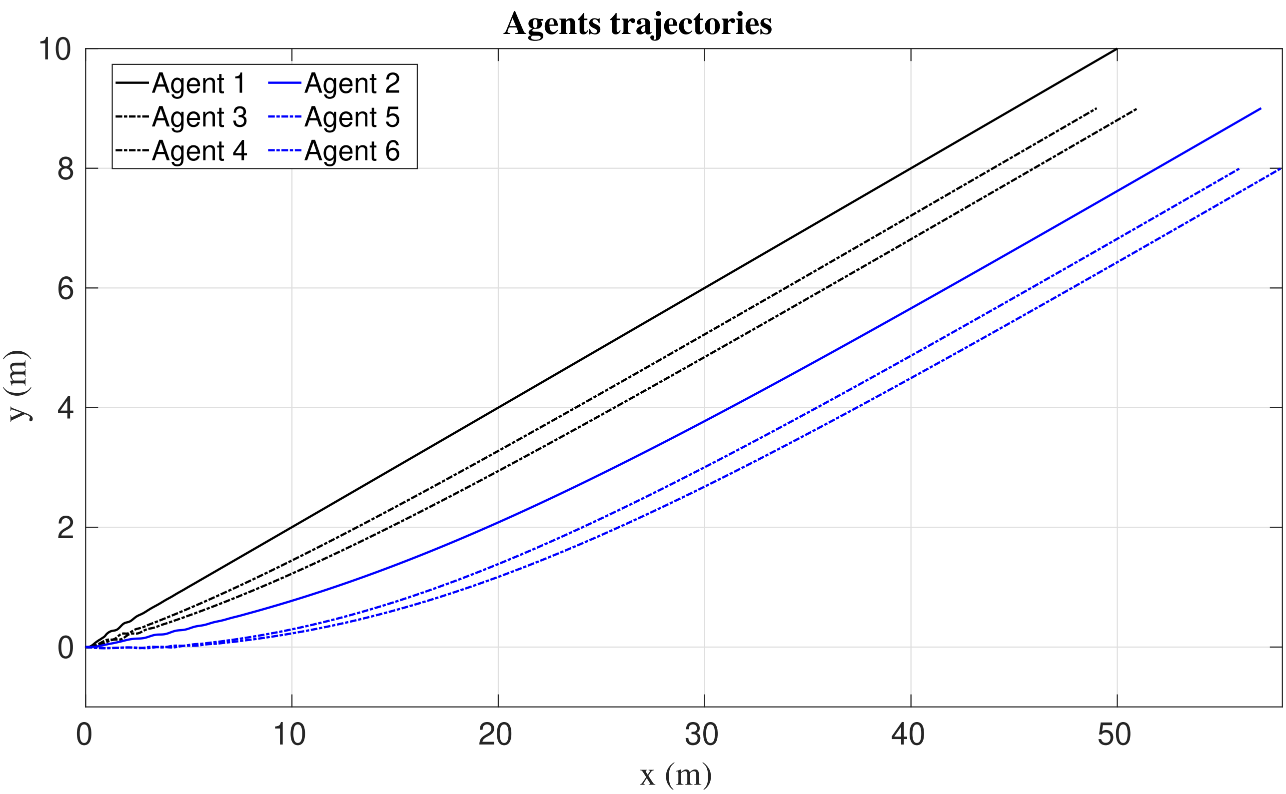

Figure 4. Agents' trajectories.

A similar analysis is conducted by examining the position and velocity error curves, in Fig. 5. It can be observed that the errors of all UAVs in the formation converge to zero. In the beginning of the simulation, we also see an oscillatory behavior on the lateral movement (y direction), which is a result of the rotors' inclination movement.

The propellers' force and the rotors' inclination torque of all UAVs in the formation were analyzed, and they are presented in Fig. 6 and 7. It can be verified that all forces and torque remained within the saturation limitations. As in Fig. 5, in the forces and torques figures, there is an oscillation at the begging of the simulation caused by the inclination of the rotors.

The results show that the formation control developed in this work, the PID altitude controller, the GSTSMC attitude, and rotors' inclination controllers effectively handle the nonlinear and coupled dynamics. This robust control system achieved the desired performance and stability in the multi-UAV formation.

5. CONCLUSIONS

We developed a formation control system based on the leader-follower and consensus approaches, whose gains were designed using the H_∞ methodology. The model of the UAVs were simplified for the control design. A previous altitude, attitude, and rotors' inclination control systems were used in the analysis of the simulations. The formation structure proposed for the simulation was composed of two virtual leaders that were responsible for governing two groups of UAVs. The results showed that the control system proposed guarantees the system's stability. For future works, we intend to consider communication faults between the virtual leader and the UAV during formation control development.

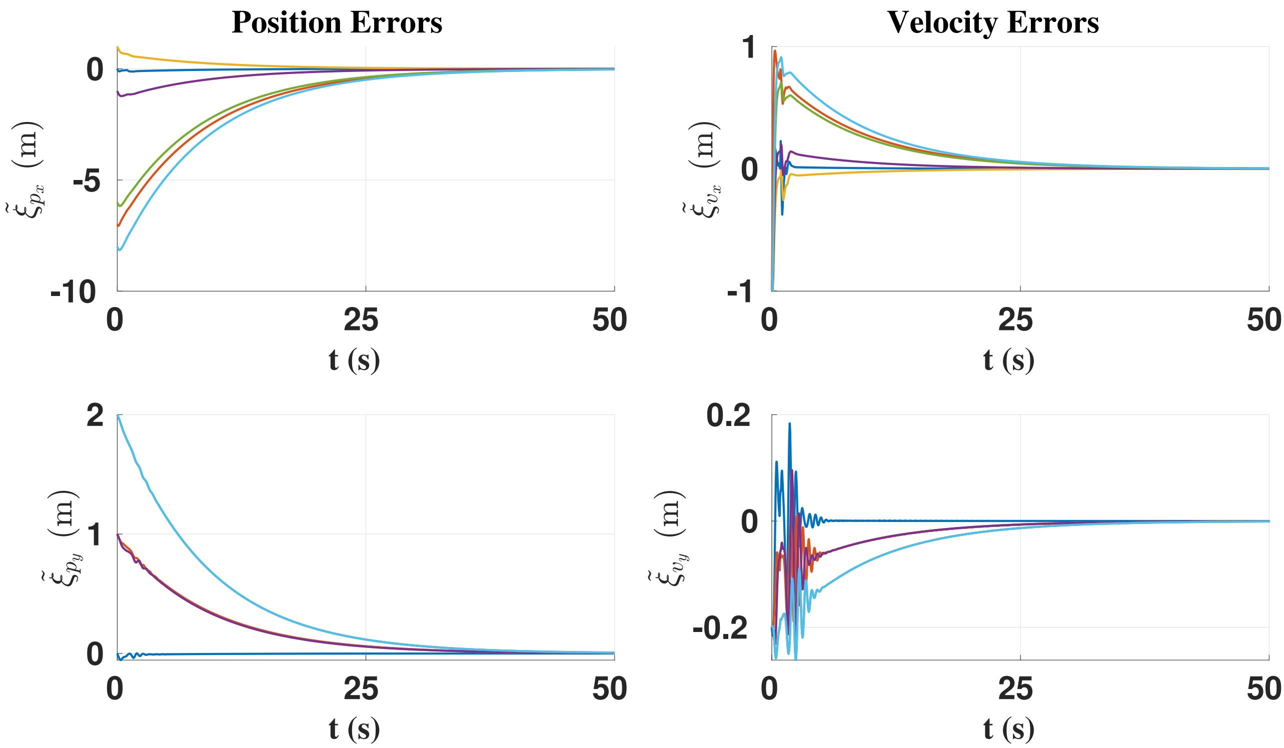

Figure 5. Position and velocity errors.

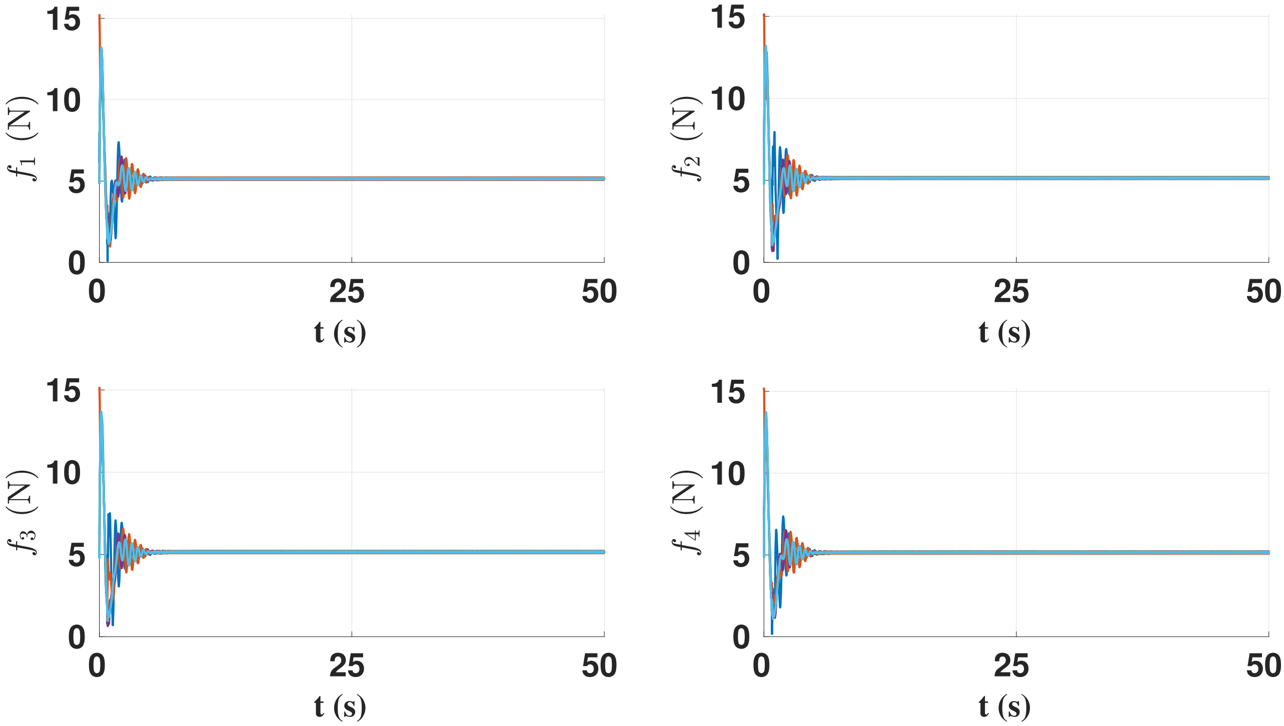

Figure 6. Propellers' force.

6. ACKNOWLEDGEMENTS

This work was supported by the Brazilian institutions of coordination of the improvement of higher education personnel and the national council for scientific and technological development.

7. REFERENCES

Ahn, H.S., 2020. *Formation control*. Springer.

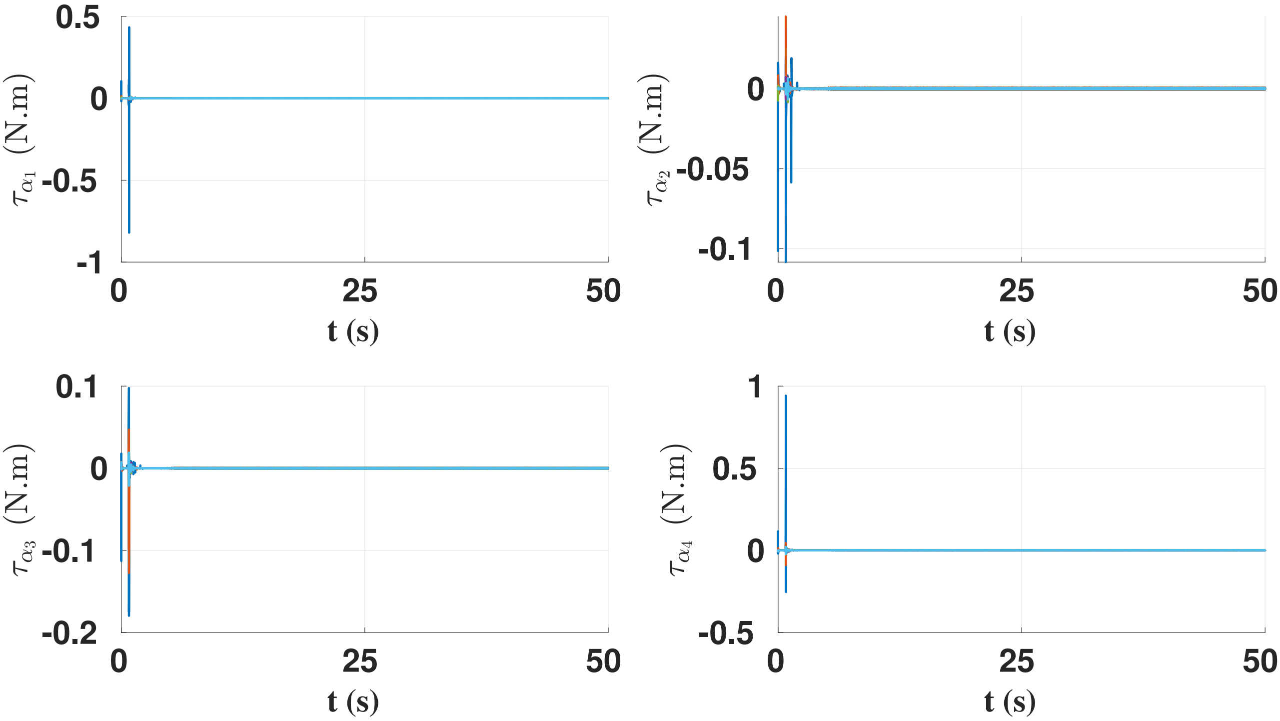

Figure 7. Rotors' torque.

Ai, X. and Yu, J., 2019. "Flatness-based finite-time leader–follower formation control of multiple quadrotors with external disturbances". *Aerospace Science and Technology*, Vol. 92, pp. 20–33.

Costa, T.L., Vendrichoski, J.C., El'Youssef, E.S. and De Pieri, E.R., 2021. "Robust control of unmanned aerial vehicle with tilt rotors and camera". In *32nd Congress of the International Council of the Aeronautical Sciences (ICAS)*.

Costa, T.L., Vendrichoski, J.C., El'Youssef, E.S. and De Pieri, E.R., 2019. "Modeling and control of an unmanned aerial vehicle with tilt rotors equipped with a camera". In *2019 19th International Conference on Advanced Robotics (ICAR)*. IEEE, pp. 1–6.

Dong, X., Li, Y., Lu, C., Hu, G., Li, Q. and Ren, Z., 2018. "Time-varying formation tracking for uav swarm systems with switching directed topologies". *IEEE transactions on neural networks and learning systems*, Vol. 30, No. 12, pp. 3674–3685.

Dong, X., Zhou, Y., Ren, Z. and Zhong, Y., 2016. "Time-varying formation tracking for second-order multi-agent systems subjected to switching topologies with application to quadrotor formation flying". *IEEE Transactions on Industrial Electronics*, Vol. 64, No. 6, pp. 5014–5024.

He, L., Bai, P., Liang, X., Zhang, J. and Wang, W., 2018. "Feedback formation control of uav swarm with multiple implicit leaders". *Aerospace Science and Technology*, Vol. 72, pp. 327–334.

Kartal, Y., Subbarao, K., Gans, N.R., Dogan, A. and Lewis, F., 2020. "Distributed backstepping based control of multiple uav formation flight subject to time delays". *IET Control Theory & Applications*, Vol. 14, No. 12, pp. 1628–1638.

Liu, H., Tian, Y., Lewis, F.L., Wan, Y. and Valavanis, K.P., 2019. "Robust formation tracking control for multiple quadrotors under aggressive maneuvers". *Automatica*, Vol. 105, pp. 179–185.

Liu, H., Wang, Y., Lewis, F.L. and Valavanis, K.P., 2020. "Robust formation tracking control for multiple quadrotors subject to switching topologies". *IEEE Transactions on Control of Network Systems*, Vol. 7, No. 3, pp. 1319–1329.

Mo, H. and Farid, G., 2019. "Nonlinear and adaptive intelligent control techniques for quadrotor uav–a survey". *Asian Journal of Control*, Vol. 21, No. 2, pp. 989–1008.

Oh, H., Shirazi, A.R., Sun, C. and Jin, Y., 2017. "Bio-inspired self-organising multi-robot pattern formation: A review". *Robotics and Autonomous Systems*, Vol. 91, pp. 83–100.

Oh, K.K., Park, M.C. and Ahn, H.S., 2015. "A survey of multi-agent formation control". *Automatica*, Vol. 53, pp. 424–440.

Vendrichoski, J.C., Costa, T.L., El'Youssef, E.S. and de Pieri, E.R., 2019. "Mathematical modeling and control of a quadrotor aerial vehicle with tiltrotors aimed for interaction tasks". In *2019 19th International Conference on Advanced Robotics (ICAR)*. IEEE, pp. 161–166.

Wang, J., Han, L., Dong, X., Li, Q. and Ren, Z., 2021. "Distributed sliding mode control for time-varying formation tracking of multi-uav system with a dynamic leader". *Aerospace Science and Technology*, Vol. 111, p. 106549.

Wu, J., Luo, C., Luo, Y. and Li, K., 2021. "Distributed uav swarm formation and collision avoidance strategies over fixed and switching topologies". *IEEE Transactions on Cybernetics*, Vol. 52, No. 10, pp. 10969–10979.

Yan, L. and Ma, B., 2020. "Distributed leader-follower formation tracking control of multiple quad-rotors". *arXiv preprint arXiv:2003.01084*.

Yang, G. and Hu, F., 2020. "Formation control of networked uavs". In *UAV Swarm Networks*, CRC Press, pp. 37–54.

8. RESPONSIBILITY NOTICE

The authors are solely responsible for the printed material included in this paper.